

GENESIS, MINERALOGY AND GEOCHEMISTRY OF KAOLIN DEPOSITS OF THE JARI RIVER, AMAPÁ STATE, BRAZIL

CÉLIA R. MONTES¹, ADOLPHO J. MELFI¹, ADILSON CARVALHO^{2,*}, ANTONIO C. VIEIRA-COELHO³ AND MILTON L. L. FORMOSO⁴

¹ Departamento de Solos e Nutrição de Plantas, ESALQ/Núcleo de Pesquisa em Geoquímica e Geofísica da Litosfera (NUPEGEL), Universidade de São Paulo (USP), Avenida Pádua Dias, 11, C.P. 09, 13418-900, Piracicaba, SP, Brazil

² Departamento de Geologia Sedimentar e Ambiental do Instituto de Geociências/NUPEGEL, USP, Rua do Lago, 562, 05508-900, São Paulo, SP, Brazil

³ Departamento de Química Industrial/LMPSol, Escola Politécnica, USP, Avenida Lineu Prestes, 580, 05508-900, São Paulo, SP, Brazil

⁴ Centro de Estudo em Petrologia e Geoquímica, Instituto de Geociências da Universidade Federal do Rio Grande do Sul, Avenida Bento Gonçalves, 9.500, 94501-970, Porto Alegre, RS, Brazil

Abstract—Kaolin samples from the Jari deposit (Amazon region) were studied using various techniques to characterize its structural and crystallochemical aspects, and to establish its origin and evolution. A profile 60 m thick was selected in a kaolin mine (Morro do Felipe) located at the banks of the Jari river. Despite the great thickness of the deposit and the variety of kaolin types, the mineralogical composition is rather homogeneous and is mainly kaolinite associated with gibbsite and small amounts of quartz, anatase, goethite and hematite. The field observations and the morphological analysis indicate the existence of sedimentary features throughout the whole profile except for the upper aluminous clayey layer (Belterra Clay). This is evidence that the Rio Jari kaolin deposit originated from sedimentary material, the Alter do Chão Formation. The presence of alternating clay and sandy layers is explained by sedimentation processes with great depositional energy variation. Thus, the accumulation of thick clay layers was related to a low-energy phase, and during the high-energy phases, the deposition process led to the accumulation of sandy materials, constituted essentially of quartz and showing strong textural and structural variation. Later on, periods of hydromorphy were responsible for iron removal and consequently for the bleaching of the sedimentary formation. The crystallinity data show an increase of the structural disorder toward the surface associated with an increase in the amount of structural Fe in the kaolinite. The Rio Jari kaolin deposits should be considered as having originated from kaolinitic clay sediments of the Alter do Chão formation (protore) that was submitted to intensive lateritic weathering processes.

Key Words—Amazon Region, Genesis, Geochemistry, Kaolin, Kaolinite, Mineralogy, Rio Jari.

INTRODUCTION

Lateritic formations cover ~80% of the Amazon basin. These formations were developed under humid and warm climatic conditions, on different rocks, both from the Precambrian basement and from sedimentary rocks. These laterites, formed by an intensive weathering process that probably started in the early Mesozoic, have a relatively monotonous and simple mineralogical composition (quartz, kaolinite, Fe and Al oxides and hydroxides). On the other hand, they present a complex structural organization in different pedological systems. The most important one in the area is the ferrallitic system, which corresponds to the preferential accumulation of kaolinite. Other systems also occurring are the hardened ferruginous system, related to the preferential accumulation of hematite and goethite and the hardened bauxitic system, in which there is preferential accumulation of gibbsite.

These pedologic systems, under the action of water flow, are subject to transformations, including mainly

material transfer (mobilization by dissolution and/or translocation of clay, Fe and organic material). These transformations, under certain situations, can promote the accumulation of economically important minerals that can constitute supergene ore deposits. That is the case, for instance, for the bauxite deposits of Paragominas, Trombetas and Carajás, in Pará State and the kaolin deposits of Manaus (Amazon), Rio Jari (Amapá) and Rio Capim (Pará).

The kaolin deposits of the Amazon region are the most important in Brazil and constitute one of the world's largest reserves of kaolinitic clays. At present, only a part of this kaolin is exploited, but it is expected that exploration will increase over the next few decades, as the traditional kaolin deposits such as those of Georgia in North America are exhausted.

Among the actively-mined deposits, those at Jari are outstanding, not only because of the size of the reserves (250 millions tons, DNPM, 2001), but also for the high quality of the final product, widely used in the international paper industry.

Despite its importance and the number of studies already carried out (Klammer, 1971; Suszcynski, 1975; Murray and Partridge, 1982; Silva and Duarte, 1983;

* E-mail address of corresponding author:
acarvalh@usp.br

Coura *et al.*, 1986; Lucas *et al.*, 1993; Duarte and Kotschoubey, 1994), some aspects of the genesis and mineralogy of these deposits are still not well understood.

Concerning its genesis, Klammer (1971) considered the Jari kaolin to be a sedimentary deposit, corresponding to the basal layer of the Belterra Clay. Suszczynski (1975) proposed a mixed origin for the clay layer. He considered its lower part as sedimentary clay and the upper part the result of *in situ* evolution. Pandolfo (1979), Murray (1986) and Coura *et al.* (1986) favored a sedimentary origin, mentioning, however, that weathering processes acting on the sediments, improved the kaolin ore quality. More recently, Duarte and Kotschoubey (1994) and Duarte (1995) proposed for the deposits an *in situ* supergenic origin, resulting from the alteration of the Alter do Chão sandstone. For these authors, the evolution would be polyphasic and controlled by climatic variations and also tectonic activities.

The age of the deposits is also a matter of controversy. According to Pandolfo (1979), Murray and Partridge (1982), Coura *et al.* (1986) and Murray (1986), the deposits are Pliocene in age though Duarte and Kotschoubey (1994) consider them to be upper Tertiary and Quaternary.

Finally, the information available on the mineralogy of the Jari deposit, is incomplete, particularly in relation

to the crystallographic and crystallochemical properties of its principal constituent, the kaolinite.

Therefore, the objective of the present paper is to contribute to a better genetic characterization of the kaolin deposits of Rio Jari. Techniques such as X-ray diffraction (XRD), electron paramagnetic resonance (EPR) and diffuse reflectance optical spectroscopy (DRS), were used to study the structural disorder of kaolinite and the structural defects of its impurities. These crystallographic and crystallochemical characteristics of the kaolinite are important parameters in defining its technological properties and thus its value.

In order to study the genetic relationships, samples from the Alter do Chão Formation, the parent rock of the river Jari kaolin, were analyzed.

THE STUDY AREA AND METHODOLOGY

The Rio Jari kaolin deposit is located on the outskirts of Monte Dourado, in southern Amapá State, near the frontier with Pará State (Figure 1). The ore deposit occurs over an extensive area, on the left bank of the lower Jari River, a tributary of the Amazon River and forms the lateritic cover of a group of low plateaux, with altitudes ~200 m. These low plateaux, separated by valleys cutting the sediments of the Alter do Chão Formation, are relicts of an ancient erosion surface.

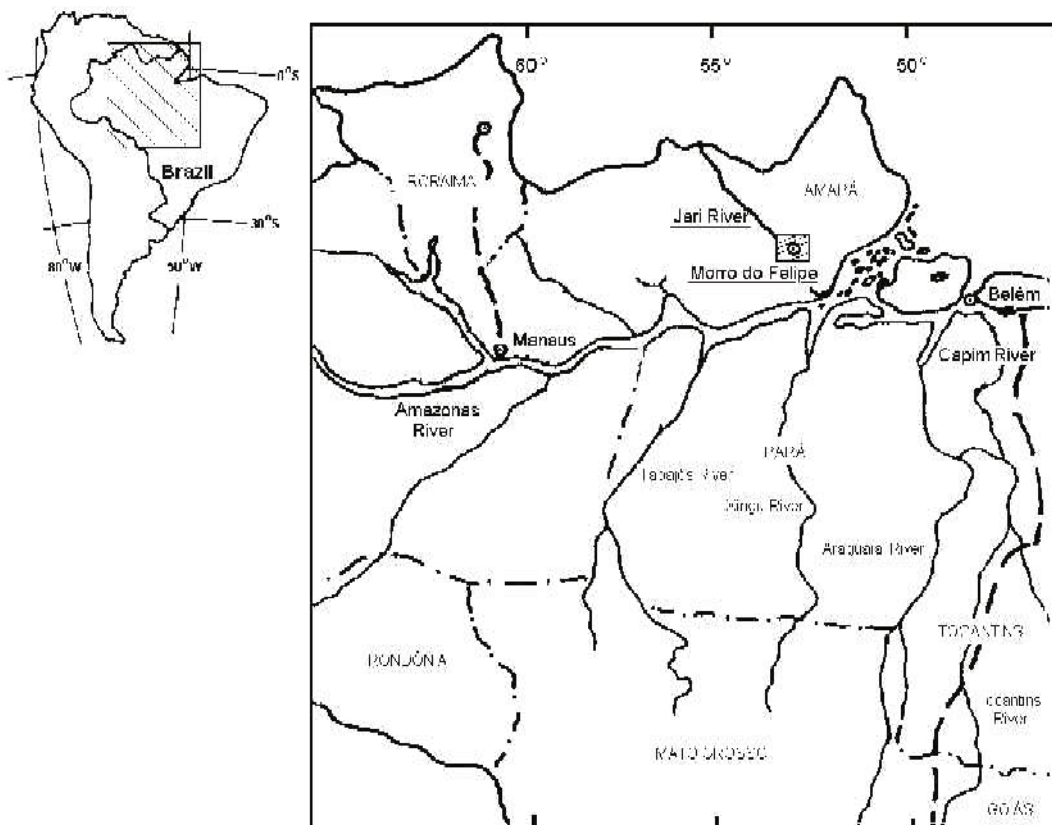


Figure 1. Map of the Amazon region, showing the study area location (Morro do Felipe).

The cross-section, selected for the fieldwork and systematic sampling, is situated in Morro do Felipe, in one of the kaolin exploration fronts of the Companhia de Mineração Caolim da Amazonia (CADAM). The total thickness of the cross-section is ~60 m, comprising 15 m of the covering Belterra Clay underlain by ~45 m of a kaolin sequence of different facies (Figure 2).

Twenty seven samples were first studied by XRD to identify the mineralogical facies and the degree of structural disorder of the kaolinites. The diagrams were obtained from random powder samples, using Philips X-Pert MPD equipment, with Cu tube and operating within the following conditions: 40 kV and 40 mA, scanning step of $0.02^{\circ}2\theta$, accumulation time of 10 s/step and spinner sample support at 30 rpm. A monochromatic filter was used to eliminate $K\beta$ radiation.

Six samples, representative of the different facies of the deposit were selected for chemical and complementary mineralogical analysis. The total chemical composition was determined by inductively coupled plasma mass spectrometry (ICP-MS), after a fusion process. The complementary mineralogical analyses were carried out by means of specific techniques such as scanning electron microscopy (SEM), optical DRS and EPR.

The SEM images were obtained using a Jeol JSM-T330A electron microscope operating within the range of 15 to 30 kV. Two types of samples analyzed were: fragments and sedimented material on a glass slide from aqueous dispersion ($H_2O + NH_4OH$).

Diffuse reflectance spectroscopy was used to determine the existence of crystalline and non-crystalline phases containing Fe associated with the kaolinites. The equipment used was a double beam Varian Cary 2300, operating in the UV–Vis–NIR region (range $33333–6667\text{ cm}^{-1}$ or 300–1500 nm) and equipped with an integrating sphere internally coated with Halon. The samples were analyzed as non-compact powder placed in a 2 mm deep sample holder. The experimental data were treated using the Kubelka-Munk theory and the results are presented as remission function (Calas, 1986).

Finally, EPR was utilized to detect any isomorphic replacement of Al^{3+} by Fe^{3+} in the kaolinites and the presence of structural defects caused by radiation. Two types of signal were observed. The first, Fe_{II} , indicates the presence of well-ordered kaolinites, with few stacking defects. The second, Fe_I , suggests the presence of Fe in disordered zones of kaolinite crystals (Meads and Malden, 1975; Gaite *et al.*, 1993; Muller and Calas, 1993; Balan, 1995). The EPR spectra were obtained from powder samples, by means of a Brucker spectrometer ERS 300E, operating in the X band (frequency ~9 GHz), with the magnetic field (H) ranging from 0 to 4000 G.

The degree of structural disorder of the kaolinites was evaluated on the basis of different crystalline indexes obtained from the XRD curves. Three methods were used

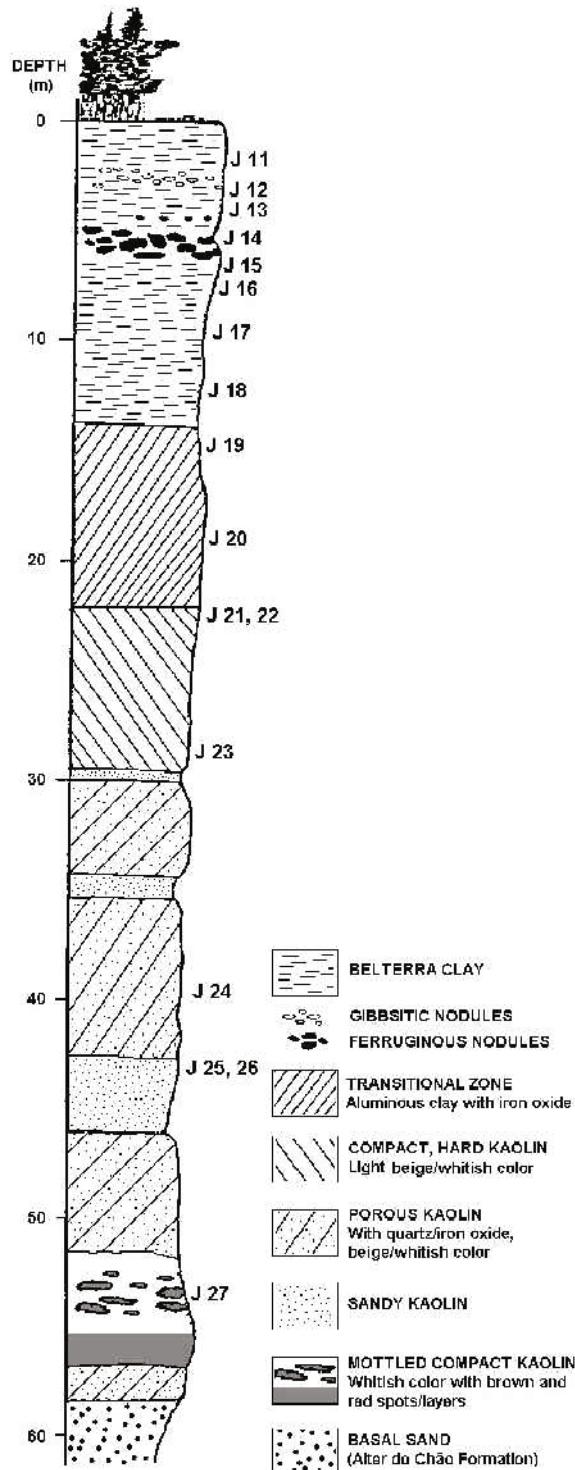


Figure 2. Typical cross-section of Morro do Felipe mine, showing the sampling sites (J 11 to 27) (adapted from Coura *et al.*, 1986).

in this study to determine the indexes. The first, the Hinckley index (Hinckley, 1963; Plançon *et al.* 1988; Galán *et al.*, 1994; Delineau, 1994), is particularly

sensitive to random translations of $nb/3$ between adjacent layers. The second, the Liétard method (R2 index) (Cases *et al.*, 1982; Galán *et al.*, 1994; Delineau, 1994), is complementary to the Hinckley index and is sensitive only to small random defects (mainly position variation of the octahedral hole). The third is the Plançon method (expert system) (Plançon *et al.*, 1988; Plançon and Zacharie, 1990; Delineau, 1994), which comprises a quantitative analysis of the different types of structural defects.

RESULTS AND DISCUSSION

Alter do Chão Formation: parent rock of the Rio Jari kaolin

The occurrence of kaolinitic clays in the Amazon region, including the Rio Jari deposit, is closely associated with the sedimentary rocks of the Alter do Chão Formation.

According to Putzer (1984), the Alter do Chão sediments consist of continental clastic deposits, slightly consolidated, comprising mainly quartz and kaolinite, associated with small amounts of Fe and Ti oxides. The formation is described as sandy clays and red kaolinitic clays, with important sandy intercalation. Its deposition dates from the Cretaceous (Daemon, 1975) and could be extended up to Tertiary (Putzer, 1984). According to Caputo (1984), the Alter do Chão Formation consists mainly of clayey sand.

The typical topography in the zones where the Alter do Chão Formation occurs, is characterized by the presence of plateaux, slightly carved, with altitudes varying from 100 to 180 m. These plateaux represent an old residual planation surface, dated as Plio-Pleistocene (Velhas Surface), with a slope of 1 to 5° towards the Amazon river valley. The dissection is related to an epeirogenetic uplifting, begun during the Pleistocene (Klammer, 1978).

In the studied area there are very few outcrops of the Alter do Chão sediments and it is, for the most part, deeply weathered, making detailed characterization difficult. In any case, it was possible to see weathered clayey sand with abundant clay intercalation. Its structure is characterized by the presence of cross bedding and quartz-pebble layers. Considering the mineralogical composition, quartz is dominant, associated with kaolinite and white mica and small amounts of Fe oxides.

As detailed characterization of the parent rock was necessary to establish its relationship with the kaolin deposits, occurrences of the Alter do Chão Formation in other areas of the Amazon region were studied. The fieldwork carried out in different areas of Pará and Amazon States, allowed us to establish the main depositional features of these sediments. These observations refer mainly to profiles studied in road cuttings and outcrops occurring near the river Negro (Montes-Lauar *et al.*, 1997).

In these regions, the rocks of the Alter do Chão Formation present, when fresh, a purple-red color and can also have intercalated layers with pale or even whitish colors. The light hues become more abundant towards the north, and their origin is attributed by Montes-Lauar *et al.* (1997) to hydromorphic phenomena. The phenomena might have been induced by a recent tectonic event that affected the original Alter do Chão sediments. The main stratigraphic aspects were observed in a 30 m thick cutting (Figure 3) that exhibits the most important depositional and post-depositional features of the sediments.

In Figure 3, four sedimentary sequences underlay a 7 m thick clayey Red Yellow Latosol which is normally referred to as the Belterra Clay (Montes-Lauar *et al.*, 1997). The lower sequence (IV), situated at the profile base, comprises a succession of coarse sand and gravel, with cross-bedding, intercalated with clayey layers that become dominant upwards. In this sequence pale horizons with horizontal stratification occur intercalated within red sand deposits with cross-bedding. In the richer clay part of this sequence, a very clay-rich dark red paleosol was observed, evidence of a sedimentation hiatus. Sequence III begins with a thin sand layer, capped by millimetric cerianite concentrations. Upwards, a thick horizon packed with coarse-grained material is seen, followed by a succession of plane-parallel strata of clayey sandstone. At the top, the clay content is greater, indicating oscillation of periods of high and low energy. Sequence II, relatively more homogenous, is thicker and comprises a succession of purple-red sandy horizons, sandy clay horizons with cross-bedding and clay layers, cut locally by sand lenses with clay pebbles. This deposition indicates a succession of periods of high energy, followed by periods of low energy, preceding the clay deposition and again a period of high energy that affected the deposited layer, breaking it down and transporting it. Finally, sequence I is homogenous and comprises coarse-grained sand and gravel deposits, colored by Fe oxide.

The mineralogical composition (Figure 3) shows that quartz and kaolinite are the most abundant minerals, associated with small amounts of Fe oxides (hematite and goethite). Accessory minerals observed were zircon, tourmaline, rutile and anatase, the last one clearly being secondary.

In the sedimentary sequence, quartz is the most abundant mineral (75–80%) except for the clayey layers where kaolinite dominates, reaching 40%.

The size of the quartz crystals is extremely variable, ranging from silt to gravel, with fine and medium sand being the most common. Despite being rather resistant to weathering, its crystals show the effects of supergene alteration, characterized by the presence of corrosion gulls and dissolution features (Figure 4).

The kaolinite, when observed with SEM, is present as rounded aggregates of small dimension (~5 µm)

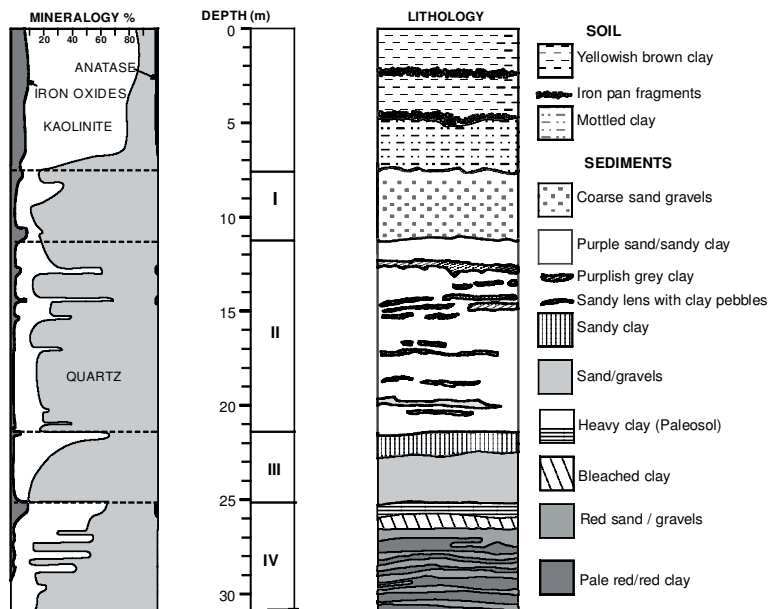


Figure 3. Cross-section showing the main stratigraphic aspects of the Alter do Chão Formation (modified from Montes-Lauar, 1997).

(Figure 5). Locally, small booklets of kaolinite can be observed, with sizes $>7\text{ }\mu\text{m}$ (Figure 6). Application of the Plançon and Zacharie expert system (Table 1) shows that the Alter do Chão sediment samples comprise a mixture of two kaolinite phases, with a high relative percentage (47–64%) of well-ordered kaolinite.

The kaolinitic phase with the high degree of disorder is considered to have originated from a previous lateritic weathering process, similar to that responsible for the formation of the paleosol. On the other hand, the well-ordered kaolinite phase is probably related to post-depositional transformation associated with the diagenetic process. The kaolinitic booklets originated from the transformation of primary minerals (mica?) that account for the first enrichment of kaolinite.

Goethite and hematite appear as subordinate mineral phases with contents generally very low, locally up to

10%. This is not the case for the upper pedological horizon, where the values are rather constant (Figure 3).

The removal of Fe oxide by the citrate-bicarbonate-dithionite (CBD) method showed that almost all the analyzed Fe is in the form of free oxide/hydroxide, crystallized as goethite or hematite coating quartz and/or kaolinite crystals.

The EPR spectra obtained in samples corresponding to the upper part of sequence IV, including the paleosol (Figure 7), shows a variation of Fe signal in kaolinite structures. The data indicate that the structural order is associated with the Fe contents. Thus, the paleosol having 9.9% Fe_2O_3 has low structural order, while the bleached clay layer, with 2.0% Fe_2O_3 , has high structural order. This suggests that kaolinite crystallization, or at least part of it, occurred during or even after Fe remobilization.

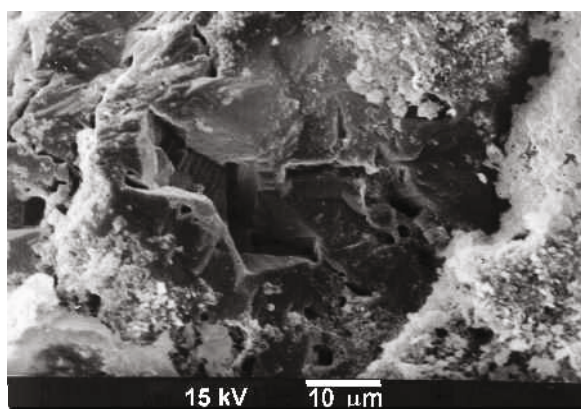


Figure 4. SEM image of quartz grains showing corrosion features (Alter do Chão Formation).

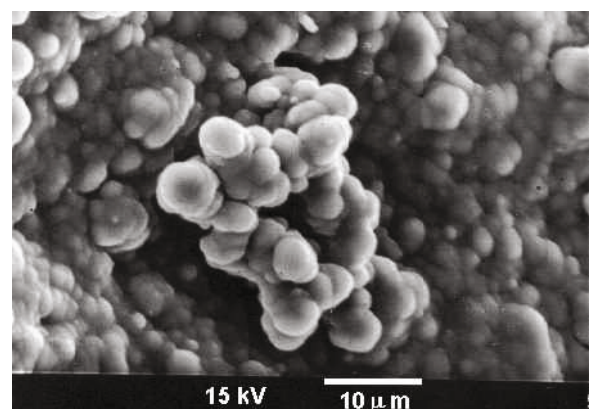


Figure 5. SEM image showing rounded kaolinite aggregates of small dimensions (Alter do Chão Formation).

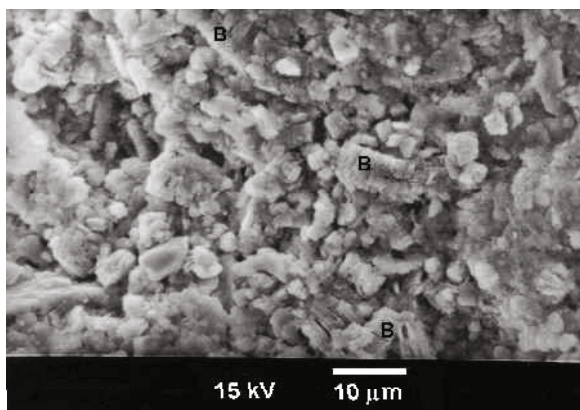


Figure 6. SEM image showing kaolinite booklets (B) in Alter do Chão sediments.

Rio Jari kaolin: geochemical and mineralogical aspects

The profile studied (Figure 2) shows weathered Alter do Chão sandy sediments in the lower part. Overlying these sediments a clay layer nearly 40 m thick occurs, consisting essentially of two horizons, separated by a 3 m thick sandy layer.

The upper part, nearly 20 m thick, comprises grayish-white compact kaolin and porous and granular compact kaolin, together with a breccia and sandy kaolin (up to 30% sand), cut by a network of joints and fissures (better quality kaolin).

The lower part, ~13 m thick, consists of a mottled kaolin with Fe oxides, showing brown spots distributed within the layer and a brown clay layer intercalated at the base.

Overlying the whole clay layer there is a transitional zone, ~8 m thick, consisting of aluminous-kaolinitic clay of pinkish light-brown color, due to the presence of Fe oxides.

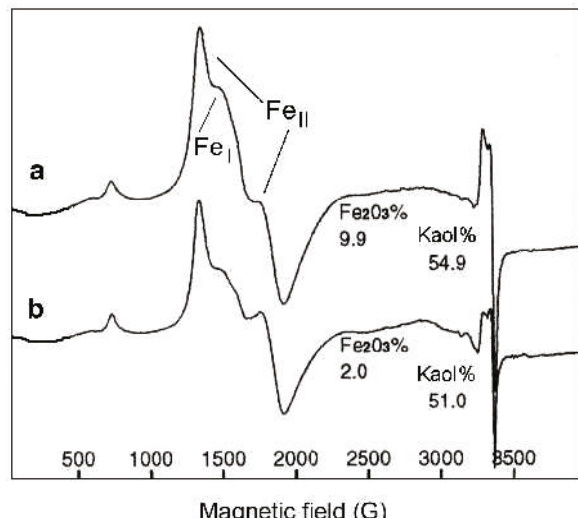


Figure 7. EPR spectra for samples of: (a) paleosol and (b) kaolin material in Alter do Chão Formation (sequence IV cf. Figure 3). (Kaol = kaolinite).

Above this transitional zone a thick aluminous clay cover, known as the Belterra Clay is found, with a red yellow color due to the presence of a large amount of Fe oxides.

The mineralogical composition of the kaolinitic layers (samples J 19 to J 27, Figure 2) is rather homogenous, kaolinite largely being dominant, followed by quartz, anatase, goethite and hematite. Gibbsite is rare and appears as traces.

In the upper part of the profile, the samples corresponding to the Belterra Clay, show kaolinite and gibbsite as essential minerals, associated with quartz, anatase and Fe oxides.

The chemical composition (wt.%) of samples from Morro do Felipe Mine profile, shown in Table 2, reflects the mineralogical homogeneity of the kaolin body.

Table 1. Experimental results of application of four methods for estimating defects in kaolinite samples from Morro do Felipe Mine profile (J 11 – Belterra Clay, J 19 and J 20 – transitional zone, J 23 to J 27a – white kaolin) and from Alter do Chão (AC) sediments.

Sample	HI	R2	Expert system of Plançon and Zacharie				
			Phase	%Idp	M	Wc	δ
J 11	–	0.55	–	–	–	–	–
J 19	0.21	0.68	1	–	54	0.01	0.04
J 20	0.27	0.78	1	–	53	0.01	0.03
J 23	0.22	0.75	1	–	53	0.01	0.03
J 24	0.38	0.78	1	–	50	0.00	0.03
J 27a	0.36	0.77	1	–	52	0.00	0.04
AC 1	1.29	0.92	2	47	–	–	–
AC 2	1.52	1.03	2	64	–	–	–
AC 3	1.44	0.93	2	59	–	–	–

AC 1 and 3 – Fe-rich sediment; AC 2 – Fe-depleted sediment; % Idp – relative percentage of low-defect kaolinite, M – average layer number in the coherent domains along the c axis, Wc – percentage of layers with vacant octahedral position; δ - small random translations between adjacent layers; p – great translation defects between adjacent layers, HI – Hinckley index; R2 index – Liètard method.

Table 2. Chemical composition (wt.%) of samples from Morro do Felipe Mine profile (J 11 – Belterra Clay, J 19 and J 20 – transitional zone, J 23 to J 27a – white kaolin, J 27b – ferruginous kaolin).

Sample	SiO ₂	Al ₂ O ₃	Fe ₂ O ₃	MgO	CaO	Na ₂ O	K ₂ O	TiO ₂	P ₂ O ₅	LOI	Total
J 11	24.26	44.99	6.30	0.03	0.06	0.03	0.03	3.17	0.04	21.59	100.49
J 19	44.08	38.24	2.07	0.01	0.01	0.02	0.01	1.39	0.05	14.32	100.20
J 20	44.63	37.97	1.97	0.01	n.d.	0.02	n.d.	1.55	0.05	14.23	100.48
J 23	45.46	37.30	2.00	n.d.	n.d.	0.01	n.d.	1.49	0.06	14.23	100.56
J 24	45.26	36.92	1.97	0.02	n.d.	0.02	0.02	1.39	0.13	14.23	99.96
J 27a	44.38	34.38	1.80	n.a.	n.a.	n.a.	n.a.	1.40	n.a.	n.a.	81.96
J 27b	39.52	31.64	14.48	0.02	0.01	0.02	n.d.	1.41	0.06	12.78	99.95

n.d. – not detected; n.a. – not analyzed

The chemical analysis can be used to estimate the mineralogical composition of the studied samples. The results obtained for the samples J 19 to J 27 show that the kaolinite content is ~80%, while quartz reaches a maximum of 15%. Anatase and Fe oxides present values of 3 to 4%. The sample J 27 is rather heterogeneous, with red areas (J 27b) in the middle of the white kaolin (J 27a). The red areas are strongly ferruginous (nearly 15% Fe₂O₃) and rich in hematite and goethite. The surrounding white kaolin is Fe-poor (~1.8%). The CBD treatment of the low-Fe samples (J 19 and J 23 to J 27a)

has shown that most of the Fe (~80%) is not removed (free Fe/total Fe ratio <20%). This suggests that some of the Fe is within more stable mineral structures, probably kaolinite. A similar situation occurs with the red areas, despite the fact that the ratio is rather high (~90%).

The analysis by SEM shows that kaolinite forms a fine matrix and like the Alter do Chão samples, occurs as rounded micro-aggregates, with diameters of ~1 µm or even less (Figure 8a). Observation of samples dispersed in water + NH₄, shows that these aggregates comprise

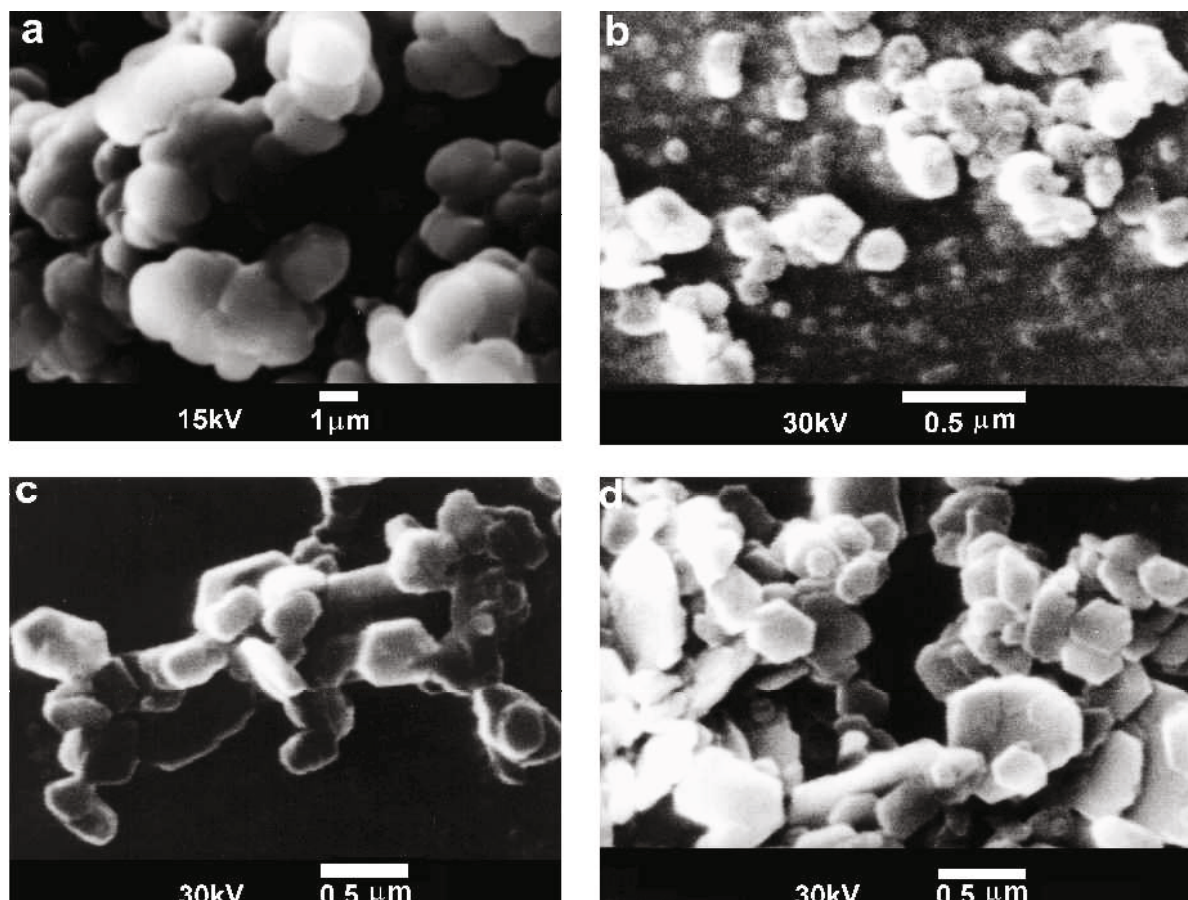


Figure 8. SEM image of kaolin from the Rio Jari deposit showing: (a) rounded kaolinite micro aggregates and (b, c, d) pseudo-hexagonal euhedral to sub-euhedral forms.

pseudo-hexagonal, euhedral to sub-euhedral kaolinite crystals, generally $<0.5\text{ }\mu\text{m}$ in size (Figure 8b,c,d).

The experimental results obtained by applying the three methods for estimating the structural order/disorder of the kaolinites are shown in Table 1. The samples of kaolinite from Morro do Felipe Mine, Rio Jari were studied and compared with the samples of clay layers from the Alter do Chão sediment.

It was not possible to apply the Hinckley and Plançon and Zacharie methods to sample J 11, from the Belterra Clay. The sample is very rich in Fe phases and gibbsite, and the 02,11 bands were not well resolved. On the other hand, the R2 index was calculated for all the samples from Jari. Sample J11 shows an R2 value less than the others. Nevertheless, despite the increase in the degree of structural order from the Belterra Clay layer down to the kaolin layers (corresponding to an increase of R2 values), a high degree of disorder along the *ab* plane still persists. This fact is confirmed by the small values of the Hinckley index for these samples. In the same way, the values of the Hinckley and Liètard indexes for the Jari samples, when compared with those of the Alter do Chão, show a higher structural order for the kaolinites in the sediments (Table 1).

By applying the Plançon and Zacharie expert system to the Jari samples, it was observed that only one kaolinite phase is present, as opposed to the samples of the Alter do Chão clay which consists of a mixture of two kaolinite phases (Table 1). With regard to the degree of crystallinity, this phase is similar to the less-ordered phase of the Alter do Chão clay sediment. On the other hand, the disappearance of the well-ordered kaolinite and the increase in kaolinite concentration in the Jari material, could be evidence that the Jari kaolinites result from dissolution of minerals (quartz and kaolinites) from the Alter do Chão sediment and their reprecipitation.

In an EPR study of the Jari samples (Figure 9), the two signals Fe_{I} and Fe_{II} , observed for the Alter do Chão sediments, were also found. The Fe_{I} signal decreases while the Fe_{II} signal increases in intensity. This proves that the structural order of kaolinite crystals in the kaolin assemblage (J 23 to J 27) and in the transition (J 19 and J 20) is better than that of the Belterra Clay (J 11), with less replacement of Al^{3+} by Fe^{3+} . In the EPR spectra, the Rio Jari kaolin samples also show signals related to radiation defects in the kaolinite. These signals increase in intensity with depth, which would indicate a higher concentration of structural defects in the kaolinites occurring in the lower part of the profile. There is an apparent contradiction, *i.e.* kaolinites with better structural order present a higher degree of radiation defects. This was explained by other authors (Muller and Calas, 1993; Muller *et al.*, 1991) as due to the fact that the basal kaolinite would be older than the upper one and consequently, the basal kaolinite would be submitted to solutions containing radioactive elements for a longer period. Actually, these solutions could contain low

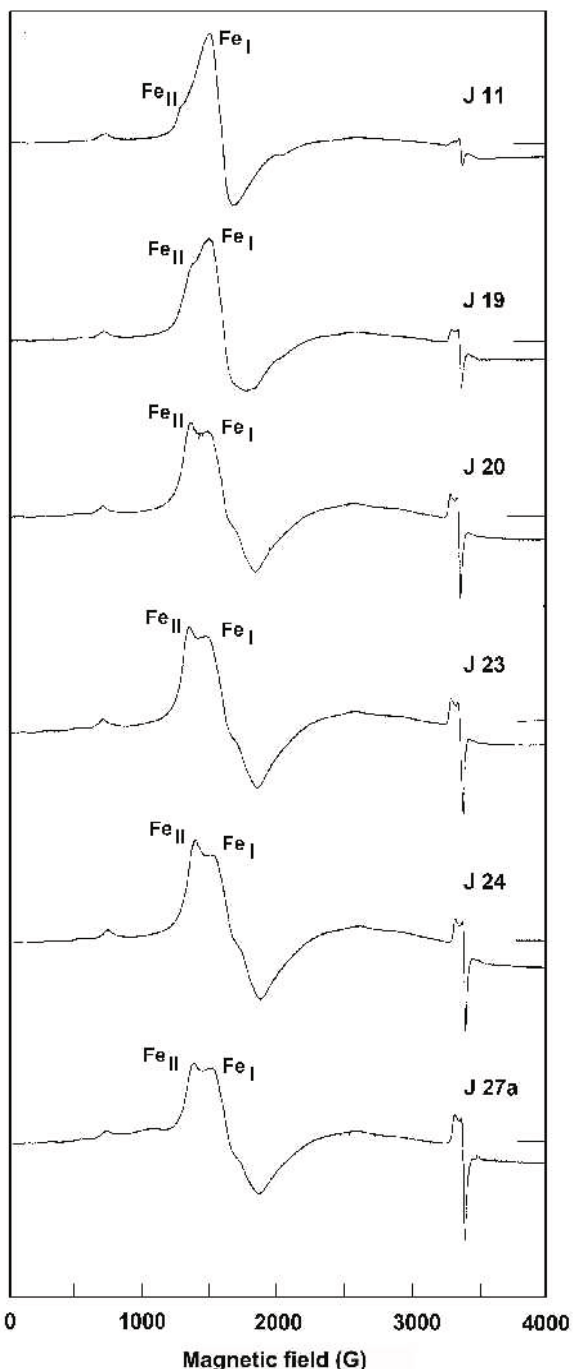


Figure 9. EPR spectra for samples from the Rio Jari deposit (*cf.* Figure 2).

concentrations of radioactive elements, as would be the case for percolation solutions or even the water table.

The different ferruginous phases were identified by using DRS (Figure 10). Goethite, despite its small amount, indicated by its low characteristic band, is always present in the kaolin. Hematite was found occasionally, in the upper part of the profile, in the transition zone to the

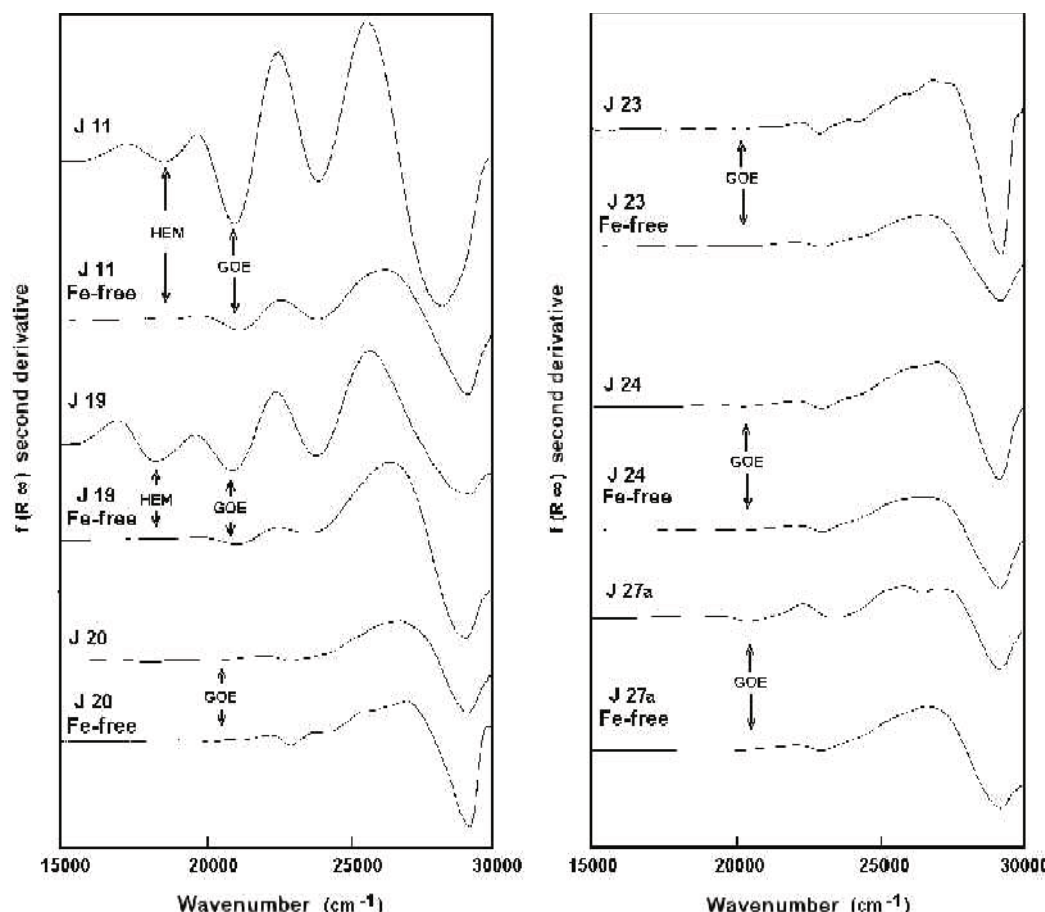


Figure 10. DRS spectra for samples from the Rio Jari deposit (*cf.* Figure 2). (GOE = goethite, HEM = hematite).

Belterra Clay, where it is associated with goethite and in the Belterra Clay itself. Considering the position of its characteristic bands, the goethites present in the Belterra Clay show a greater degree of replacement of Fe^{3+} by Al^{3+} ($\sim 21000 \text{ cm}^{-1}$) compared with goethites occurring in the kaolin body ($\sim 20000 \text{ cm}^{-1}$).

CONCLUSIONS

The field observations and the morphological analysis of the Rio Jari kaolin samples, indicate clearly the existence of sedimentary features throughout the whole profile, except for the upper Belterra Clay. The intercalation of sandy and clayey layers can only be explained by the action of sedimentation processes with a great variation in depositional energy. Thus, during the sedimentation of the Alter do Chão Formation, layers formed within a phase of low energy would allow the accumulation of thick clay layers, rich in kaolinite and associated with a significant amount of Fe oxides and hydroxides, and quartz. In the high-energy phases, the deposition process led to the accumulation of sandy materials, consisting essentially of quartz and showing strong textural and structural variation.

Later, the area would have been subjected to periods of hydromorphy, probably caused by tectonic events that affected the Amazon region during the Tertiary and/or Quaternary (Costa and Hassui, 1997). The hydromorphic environment would have been responsible for removal of Fe and consequently for the bleaching of the Alter do Chão Formation. Some relics of the past ferruginization of the Alter do Chão Formation can still be found in the studied material. Later, this material was subjected to an intensive lateritization process, resulting in an enrichment of the kaolin, mainly through a process of mineral dissolution and particularly of quartz. The presence of corroded quartz crystals, observed by SEM, is a sign of its dissolution. Undoubtedly, this dissolution was important, keeping a high degree of H_4SiO_4 activity in the solution (Millot and Fauck, 1971). In this condition, the lateritization of the Alter do Chão Formation led to dissolution of quartz and kaolinite and reprecipitation of a second phase of kaolinite, forming small crystals.

The crystallinity data show an increase of the structural disorder toward the surface, corresponding to a decrease of the kaolinite stabilization, as is indicated in the Belterra Clay by the presence of gibbsite, which certainly originated from the kaolinites.

The Rio Jari kaolin deposits should be considered as having originated from kaolinitic clay sediments of the Alter do Chão formation (protore) which were subjected to an intensive lateritic weathering process.

ACKNOWLEDGMENTS

This study received financial support from PRONEX and FAPESP. The authors are also grateful to Companhia de Mineração Caolim da Amazonia (CADAM) for their help during the fieldwork.

REFERENCES

- Balan, E. (1995) *Cristallochimie du Fer dans les Kaolinites. DEA de Géochimie Fondamentale et Appliquée*. Université Paris VII et IPGP, Paris, France, 29 pp.
- Calas, G. (1986) *Méthodes Spectroscopiques Appliquées aux Minéraux*. Société Française de Minéralogie et Cristallographie, Paris, 426 pp.
- Caputo, M.V. (1984) Stratigraphy, tectonics, paleoclimatology and paleogeography of northern basins of Brazil. University of California, Santa Barbara. Ph.D. thesis, 583 pp.
- Cases, J.M., Liétard, O., Yvon, J. and Delon, J.F. (1982) Étude des propriétés cristallochimiques, morphologiques, superficielles des kaolinites désordonnées. *Bulletin Minéralogique* **105**, 439–455.
- Costa, J.B.S. and Hassui, Y. (1997) Evolução Geológica da Amazônia. Pp. 16–90 in: *Contribuições à Geologia da Amazônia* (M.L. Costa and R.S. Angélica, editors). FINEP/SBG Núcleo Norte, Brazil.
- Coura, F., Moeri, E.N. and Kern, R.S. (1986) Geologia do Caolim do Jari. *Anais do XXXIV Congresso Brasileiro de Geologia, Goiânia*, **5**, 2248–2258.
- Daemon, R.F. (1975) Contribuição à datação da Formação Alter do Chão, Bacia do Amazonas. *Revista Brasileira de Geociências*, **5**, 78–84.
- Delineau, T. (1994) Les argiles kaoliniques du Bassin des Charentes (France): analyses typologique, cristallo-chimique, spéciation du fer et applications. Thèse de doctorat. Institut National Polytechnique de Lorraine/École Nationale Supérieure de Géologie de Nancy, France.
- DNPM (2001) *Sumário Mineral 2001*. Departamento Nacional de produção Mineral, Brasília, Brasil. (www.dnpm.gov.br/sm2001.html).
- Duarte, A.L.S. (1995) Caolim do Morro do Felipe, baixo Rio Jari, Estado do Amapá. Contexto Geológico e Gênese. Dissertação de Mestrado, Universidade Federal do Pará, 132 pp.
- Duarte, A.L.S. and Kotschoubey, B. (1994) Cobertura caolinítica da região do baixo Rio Jari. Proposta de evolução. Simpósio de Geologia da Amazônia, SBG, 4, Belém. *Boletim de Resumos Expandidos*, 79–82.
- Gaité, J., Ermakoff, P. and Muller, J.-P. (1993) Characterization and origin of two Fe³⁺ EPR spectra in kaolinite. *Physics and Chemistry of Minerals*, **20**, 242–247.
- Galán, E., Aparicio, P., González, I. and La Iglesia, A. (1994) Influence of associated components of kaolin on the degree of disorder of kaolinite as determined by XRD. *Geologica Carpathica – Series Clays*, **45**, 59–75.
- Hinckley, D.N. (1963) Variability in 'cristallinity' values among the kaolin deposits of the coastal plain of Georgia and South Carolina. *Clays and Clay Minerals*, **13**, 229–235.
- Klammer, G. (1971) Über plio-pleistozäne terrassen und ihre sedimente im unteren Amazonasgebiet. *Zeitschrift für Geomorphologie*, **15**, 62–106.
- Klammer, G. (1978) Reliefentwicklung In Amazonas becken Und Plio-Pleistozaene Bewegungen Des Meeresspiegels. *Zeitschrift für Geomorphologie*, **22**, 390–416.
- Lucas, Y., Luizão, F.J., Chauvel, A., Rouiller, J. and Nahon, D. (1993) The relation between biological activity of the rain forest and mineral composition of soils. *Science*, **260**, 521–523.
- Meads, R.E. and Malden, P.J. (1975) Electron spin resonance in natural kaolinites containing Fe³⁺ and other transition metal ions. *Clay Minerals*, **10**, 313–345.
- Millot, G. and Fauck, R. (1971) Sur l'origine de la silice de silicifications climatiques et des diatomites quaternaires du Sahara. *Comptes Rendu de l'Academie des Sciences, Paris, France*, **272**, 4–7.
- Montes-Lauar, C.R., Balan, E., Fritsch, E., Melfi, A.J., Boulet, R., Magat, Ph. and Carvalho, A. (1997) Stratigraphy and mineralogy of red-purple continental sediments (Alter do Chão Formation of Manaus, Brazil). *11th International Clay Conference, Ottawa, Canada*. Abstract A-52.
- Muller, J.-P. and Calas, G. (1993) Genetic significance of paramagnetic centers in kaolinites. Pp. 261–289 in: *Kaolin Genesis and Utilization* (H.H. Murray, W. Bundy and C. Harvey, editors). The Clay Minerals Society, Boulder, Colorado.
- Muller, J.-P., Clozel, B., Ildefonse, P. and Calas, G. (1991) Radiation-induced defects in kaolinites: indirect assessment of radionuclides migration in the geosphere. *Applied Geochemistry Supplement Issues, N°1*, 205–216.
- Murray, H.H. (1986) Clays. Pp. 109–136 in: *Ullmann's Encyclopedia of Industrial Chemistry*, Vol. A7. VCH Verlagsgesellschaft, Weinheim, Germany.
- Murray, H.H. and Partridge, P. (1982) Genesis of Rio Jari kaolin. *Proceedings of the 7th International Clay Conference, Bologna-Pavia*, 279–291 (H. Van Olphen and F. Veniali, editors). Developments in Sedimentology, **35**. Elsevier, Amsterdam.
- Pandolfo, C. (1979) Bauxita, caulins e argilas na Amazônia. *Cerâmica*, **25**, 1–15.
- Plançon, A. and Zacharie, C. (1990) An expert system for the structural characterization of kaolinites. *Clay Minerals*, **25**, 249–260.
- Plançon, A., Giese Jr., R.F. and Snyder, R.N. (1988) The Hinckley index for kaolinites. *Clay Minerals*, **23**, 249–260.
- Putzer, H. (1984) The geological evolution of the Amazon Basin and its mineral resources. Pp. 15–46 in: *The Amazon: Limnology and Landscape Ecology of a Mighty Tropical River and its Basin* (H. Sioli, editor). Monographiae Biologicae, **56**. Junk Publishers, Dordrecht, The Netherlands.
- Silva, S.P. and Duarte, A.L.S. (1983) *Depósitos de caolim do Morro do Filipe, Município de Mazagão – Amapá*. Relatório no 1734, DNPM, 12 pp.
- Suszczynski, E.F. (1975) *Os recursos minerais e potenciais do Brasil e sua metalogenia*. Interciências, Rio de Janeiro, 536 pp.

(Received 26 July 2001; revised 18 January 2002; Ms. 567)